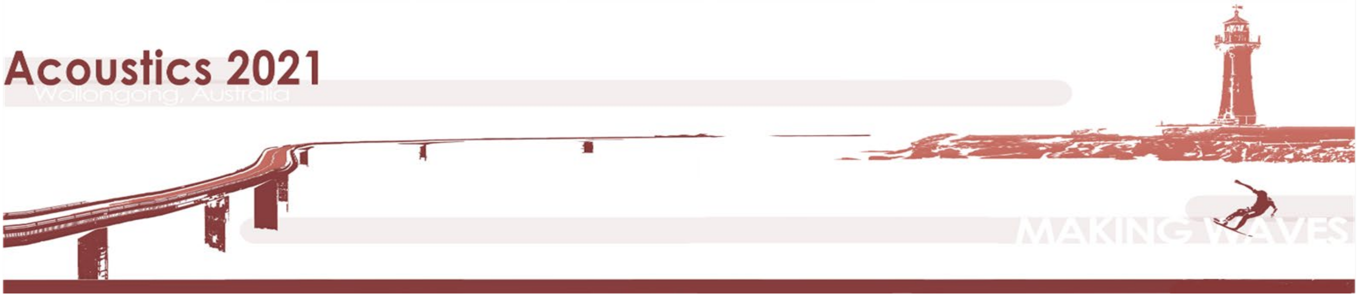

Predicting outdoor sound propagation in the presence of wind and temperature inversions

Ray Kirby

Centre for Audio, Acoustics and Vibration, University of Technology, Sydney, Sydney, Australia

ABSTRACT

It is common in Australia to encounter complex meteorological conditions such as temperature inversions, especially at night. These climatic conditions can have a significant effect on the propagation of sound, and this can influence the noise levels experienced by local communities from activities such as mining. It is, therefore, desirable to understand how the propagation of sound is influenced by climatic conditions, especially in the planning and monitoring of noise generating activities. In this article, a semi analytic finite element method is used to generate solutions to the exact governing wave equation for a two dimensional problem. This permits arbitrary wind and temperature profiles to be included, so that exact solutions can be generated for temperature inversions in the presence of wind. Predictions are presented for range independent problems in the presence of different temperature inversions, as well as ground conditions. It will be shown that the semi analytic finite element method enables solutions to be generated for large ranges, and predictions will be presented here for ranges of up to 5 km.

1 INTRODUCTION

Predicting the propagation of sound in the atmosphere presents many challenges. This includes accommodating complex environmental conditions, such as variations in temperature and wind speed, as well as the influence of the ground impedance. These factors lead to a challenging mathematical problem which is ideally addressed using numerical methods, as these can accommodate complex fluid properties. However, if one wishes to apply numerical methods such as the finite element (FE) method then the dimensions typically encountered in outdoor sound propagation mean that the number of degrees of freedom required quickly becomes prohibitive.

This means that in outdoor sound propagation it is common practice to approximate the governing wave equation and/or the underlying physics of the problem. Popular approaches include ray based models (Ostashev and Wilson, 2016), which track energy propagation and generally work best at higher frequencies, although a number of approximations are required in order to deliver predictions when complex wind profiles are present. Parabolic equations (PEs) are now one of the most widely used methods for examining outdoor sound propagation (Gilbert and White, 1989), although this approach is also approximate as it removes terms from the governing equation, and is limited to sound propagation in one direction only. However, PEs can accommodate range varying fluid properties and have been shown to provide a good approximation for relatively complex atmospheric conditions (Ostashev et al., 2020).

The approximations inherent in these models raises the question: how do we know the predictions are accurate, especially given the large number of variables present? For example, if we compare against experimental measurements can we be sure that any agreement reflects the accuracy of the model, rather than a fortuitous combinations of approximations within the model and errors in the experiment. Thus, when developing new theoretical models it is important first to understand the accuracy of the model, and to do this it needs to be benchmarked against a theoretical approach that is known to be ‘exact’ or as close to exact as possible. For outdoor sound propagation a benchmark that is often chosen is the Fast Field Program (FFP), (Taherzadeh et al., 1998, and West et al., 1991). However, this approach again includes approximations, for example by discretisation of the fluid properties in the vertical direction into laminae with constant fluid properties. This means that the nonlinear wind and temperature profiles are approximated as discontinuous functions, and wind shear cannot be included. Moreover, the method becomes progressively unstable as the gradient in the fluid properties increases (Taherzadeh et al., 1998).

To address these challenges, and to deliver a more comprehensive benchmark solution, Kirby (2020, 2021) recently developed an FE based approach for range independent problems. The method removes the need to mesh the range dimension so that discretisation is required in the height direction only. This is referred to as the semi analytic finite element (SAFE) method (see also, Duan and Kirby, 2019; Duan et al., 2016), and it radically reduces the computational size of the problem, which presents the opportunity for application to outdoor sound propagation, at least for range independent problems. Furthermore, by using FE it is possible also to include all of the physics of the problem provided the fluid is vertically stratified in two (range – height) dimensions. It was then shown that the SAFE method will deliver an exact solution of the problem provided a sufficient number of degrees of freedom are included in the FE mesh, as well as a sufficient number of normal modes (Kirby, 2020). The SAFE method is, therefore, ideally suited to delivering a benchmark prediction for complex atmospheric sound propagation problems, such as those in which a logarithmic wind velocity profile is combined with a logarithmic temperature inversion over an impedance surface. Accordingly, in this article the method is explored in more detail and new predictions are generated for complex atmospheric conditions relevant to conditions in Australia.

2 THEORY

The detailed theoretical development of the SAFE method for outdoor sound propagation is described by Kirby (2020, 2021). The method is briefly summarised here for a point source above a ground characterised by a locally reacting impedance. The governing wave equation is derived from the Navier-Stokes equation, and for a vertically stratified two-dimensional geometry, with a range (x) and a height (z), the equations of motion are (Ostashev and Wilson, 2016):

$$\mathrm{D}_t^2 \rho u_z' + \mathrm{D}_t \frac{\partial p'}{\partial z} + \frac{g}{c^2} \mathrm{D}_t p' = 0 \tag{1}$$

$$\mathrm{D}_t u_x' + \frac{\partial \mathrm{v}_x}{\partial z} u_z' + \frac{1}{\rho}\frac{\partial p}{\partial x} = 0, \tag{2}$$

$$\frac{1}{\rho c^2} \mathrm{D}_t p' + \frac{1}{\rho}\frac{\partial \rho}{\partial z} u_z' + \frac{\partial u_z'}{\partial z} + \frac{\partial u_x'}{\partial x} = Q \tag{3}$$

Here, p' is acoustic pressure, c is the speed of sound, ρ is the fluid density, $\mathbf{u}' = (u_x', u_z')$ is the acoustic particle velocity, and $\mathbf{v} = (\mathrm{v}_x, 0)$ is the velocity of the fluid. Note that fluid properties ρ, c and v_x are arbitrary functions of the height z, and the derivative of each of these properties in the x direction is zero. In addition, g is gravity, Q is a mass source, and $\mathrm{D}_t = \partial/\partial t + \mathrm{v}_x\, \partial/\partial x$, with t denoting time.

These equations of motion contain all the physics of the problem, including wind shear and the effects of gravity, although the latter is only relevant here when calculating the variation of fluid density with height. Following Ostashev and Wilson (2016), it is possible to combine these equations into a single wave equation in the acoustic pressure, which gives

$$\left[\frac{1}{c^2}\mathrm{D}_t^3 - \mathrm{D}_t\left(\frac{\partial^2}{\partial x^2} + \frac{\partial^2}{\partial z^2} + 2\tilde{g}\frac{\partial}{\partial z} + \tilde{g}^2 - \frac{2\tilde{g}}{c}\frac{\partial c}{\partial z}\right) + 2\frac{\partial \mathrm{v}_x}{\partial z}\frac{\partial}{\partial x}\left(\tilde{g} + \frac{\partial}{\partial z}\right) + \left(2\tilde{g} + \frac{1}{\rho}\frac{\partial \rho}{\partial z}\right) D_t \left(\tilde{g} + \frac{\partial}{\partial z}\right)\right] p' = \rho \mathrm{D}_t^2 Q, \tag{4}$$

where $\tilde{g} = g/c^2$ and $\rho = \frac{\rho_0 T_0}{T}\exp\left(-\frac{g}{R_a}\int_0^z \frac{1}{T} dz'\right)$. In addition, ρ_0 and T_0 are reference values for density and temperature, respectively, at a reference height $z = z_0$; and $c^2 = \gamma_a R_a T$, with γ_a the ratio of specific heats, T is air temperature, and R_a the gas constant for dry air.

This wave equation is exact for a two dimensional problem, which means that an accurate solution of this equation will deliver a true benchmark solution for range independent problems. The SAFE method proceeds by first calculating the normal modes of the open waveguide. To do this, the following ansatz is specified:

$$p'(x,z,t) = \sum_{n=1}^{\infty} \mathrm{A}_n p_n(z) e^{i\omega t - ik_0\gamma_n x}, \qquad x \geq 0 \tag{5}$$

which is then substituted into the governing wave equation, and after removing the point source Q for this part of the solution, an eigenequation is obtained that is solved for the normal modes:

$$k^2[1-\gamma \mathrm{M}]^3 p + [1-\gamma\mathrm{M}]\left\{\left(\tilde{g}^2 - \frac{2\tilde{g}}{c}\frac{\partial c}{\partial z}\right) + 2\tilde{g}\frac{\partial}{\partial z} + \frac{\partial^2}{\partial z^2} - k_0^2\gamma^2\right\} p + 2\gamma\frac{\partial \mathrm{M}}{\partial z}\left(\tilde{g} + \frac{\partial}{\partial z}\right) p - \left[2\tilde{g} + \frac{1}{\rho}\frac{\partial\rho}{\partial z}\right][1 - \gamma\mathrm{M}]\left(\tilde{g} + \frac{\partial}{\partial z}\right) p = 0. \tag{6}$$

Here, the time dependence has been removed, $k = \omega/c$, and the Mach number $\mathrm{M} = \mathrm{v}_x/c_0$. Note that Eq. (6) is a cubic equation in the wavenumber γ only if one retains the wind shear terms. If wind shear is removed then the equation returns to the more well-known convected Helmholtz equation (Kirby, 2020). Solution of Eq. (6) is achieved through the use of a weak Galerkin approach, which yields a finite element discretisation of this equation. This is then solved using an eigensolver in MATLAB® in order to obtain the normal modes propagating in the positive x direction: γ_n and $p_n(z)$; and the negative x direction: γ_{-n} and $p_{-n}(z)$.

After solution of the eigenequation it is necessary to add in a point source, which enables the amplitudes of each normal mode to be obtained. This is achieved by enforcing continuity of acoustic pressure and axial particle velocity over a vertical line passing through the point source. This yields the following expression for the modal amplitudes (Kirby, 2021):

$$\mathrm{A}_n = \frac{iq_0}{\rho_s \Lambda_{n,n}} p_n(z_s) \tag{7}$$

where z_s is the source height, q_0 is the amplitude of the source, and ρ_s is the fluid density at the source. In addition:

$$\Lambda_{m,n} = \int_0^b \frac{1}{\rho}\left\{\frac{k^2\mathrm{M}}{k_0} - \frac{\tilde{g}}{k_0(1-\mathrm{M}\gamma_n)^2}\frac{\partial \mathrm{M}}{\partial z} + \frac{k_0\gamma_n}{(1-\mathrm{M}\gamma_n)}\left[1 + \frac{i}{k_0(1-\mathrm{M}\gamma_n)}\frac{\partial \mathrm{M}}{\partial z}\right]\right\} p_m(z)p_n(z)dz. \tag{8}$$

where the finite element problem is closed at a height b using a perfectly matched layer in the region $a \le z \le b$, where $(b-a) \ll a$. Equation (7) can readily be solved for the modal amplitudes if one assumes that Eq. (8) is orthogonal, which has been shown numerically to be the case for this class of problem (Kirby, 2020, 2021). After obtaining the modal amplitudes, one then substitutes these back into Eq. (5), and with knowledge of the properties of each normal mode, the sound pressure field can be calculated after truncating the modal sum at $n = W$. Note that this sound pressure field should converge towards the exact solution as the number of elements in the mesh, and the number of modes in the modal sum, are increased.

It is common to compute the transmission loss (TL) for outdoor sound propagation problems, and this is computed by normalising the sound pressure field against the equivalent one computed for free field propagation at a distance of 1m from the point source. This eliminates the source amplitude and yields the following expression for spherical spreading (Kirby, 2021)

$$\mathrm{TL}(x,z) = 20\log_{10}\left|\sum_{n=1}^{\mathrm{W}} \frac{2p_n(z)p_n(z_s)}{\rho_s\Lambda_{n,n}\mathrm{R}\mathrm{H}_0^{(2)}(k_r\mathrm{R})} e^{-ik_0\gamma_n x}\right|. \tag{9}$$

where $\mathrm{R}^2 = z^2 + (x_r - x_s)^2$, z_r is the height of the receiver, k_r is the fluid wavenumber at the receiver, and $\mathrm{H}_0^{(2)}$ is a Hankel function of the second kind and order 0.

3 RESULTS

To demonstrate the flexibility of the SAFE method an arbitrary wind velocity and temperature profile are specified here, see Fig. 1. In Fig. 1, a logarithmic profile is specified for both the fluid temperature (Lihoreau et al., 2006) and the wind velocity (Taherzadeh et al., 1998). The temperature profile is also chosen to represent a temperature inversion, and this is achieved by combining the logarithmic profile at low altitude with a fourth order polynomial at high altitudes, and then a constant profile above 320 m. Note that these fluid properties are not attempting to replicate known atmospheric conditions, rather they are chosen to demonstrate that any combination of temperature and wind velocity profiles can be accommodated. Moreover, the use of logarithmic and polynomial profiles means that analytic expressions can easily be obtained for their derivatives with respect to the z direction.
The substitution of the fluid properties into the SAFE model enables predictions to be produced for a given frequency of excitation. The sound pressure field can then be reconstructed for the downstream direction using Eq. (5), and for the upstream direction:

$$p'(x,z) = \sum_{n=1}^{\mathrm{W}} \mathrm{A}_{-n}p_{-n}(z)e^{-ik_0\gamma_{-n}x}, \qquad x \le 0. \tag{10}$$

Here, the modal amplitudes A_{-n} are found after enforcing continuity of pressure over the line of symmetry at $x = 0$, which gives $\mathrm{A}_n p_n(z) = \mathrm{A}_{-n}p_{-n}(z)$, and then solving for A_{-n}. This then enables the pressure field to be plotted over an extend range, and so in Fig. 2 the sound pressure field is plotted over a range of 8 km.

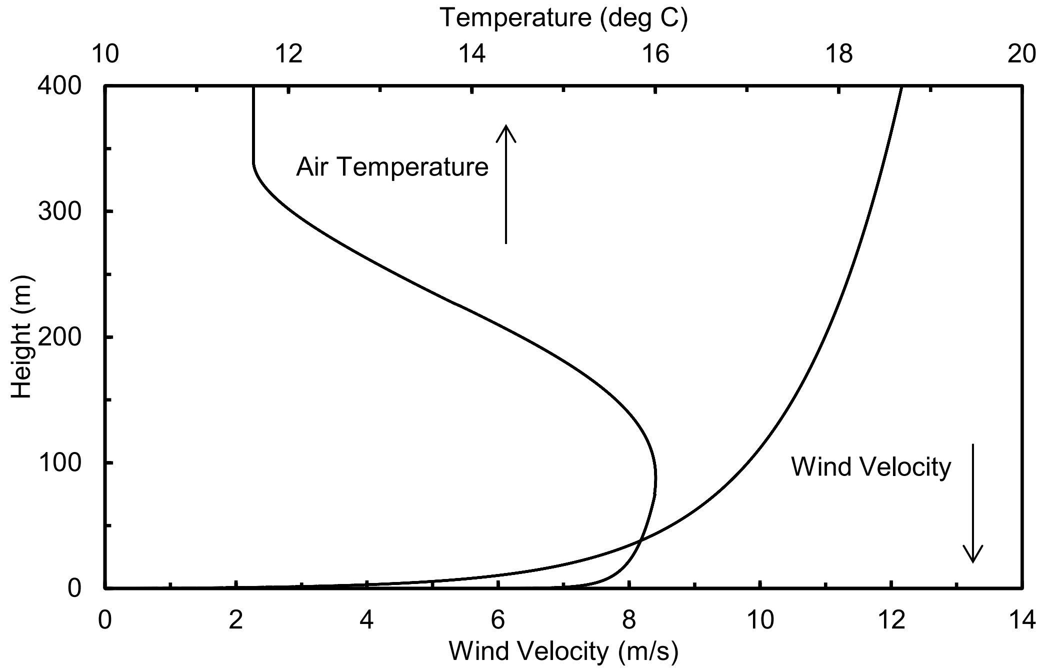

Figure 1: Fluid properties

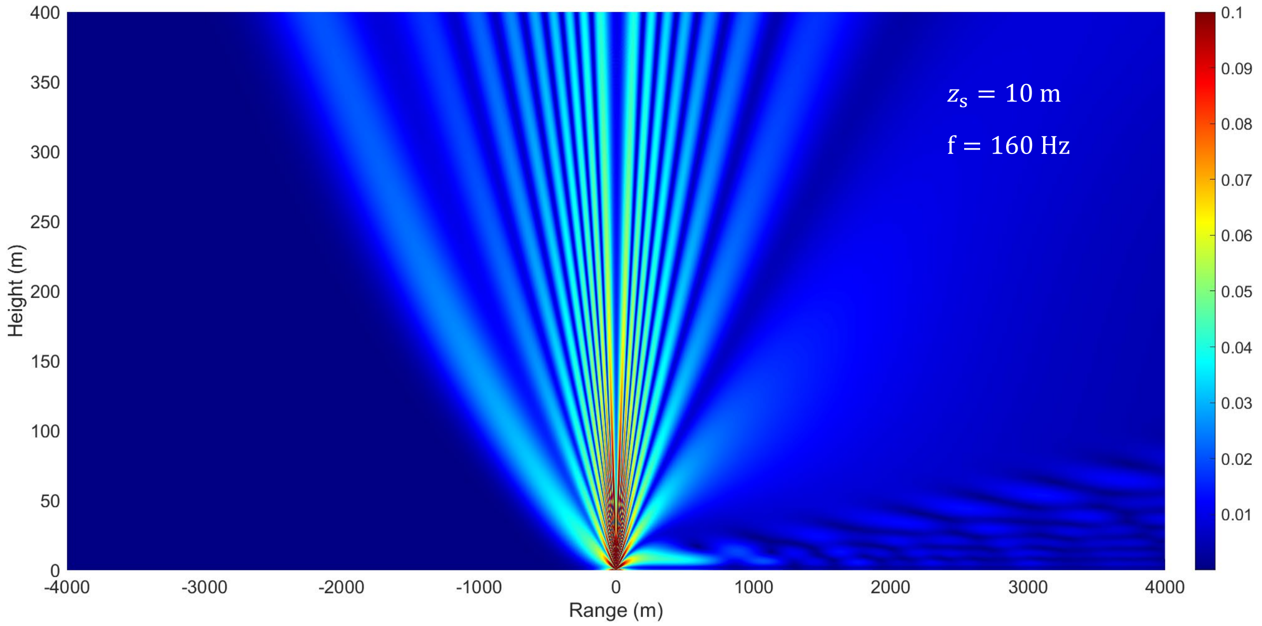

Figure 2: SAFE predictions of normalised sound pressure field at 160 Hz.

In Fig. 2 the source height is 10 m and the ground has a flow resistivity of 100 kPa s/m^2, with the impedance of the ground calculated using the model of Attenborough et al. (1995). Note that the SAFE method can readily compute sound pressure fields over long distances because the mesh is only specified over the height of the waveguide, which means the computation of values for $x \neq 0$ is simply a post-processing exercise. This was shown previously by Kirby (2020), where distances up to 100 km were studied for infrasound problems.

In principle the SAFE method can be extended to higher frequencies simply by increasing the number of finite elements and the number of modes retained in the modal sum. Accordingly, in Fig. 3 this the sound pressure field is illustrated for a frequency of 1 kHz, and here the range is reduced to 500 m in order to continue to observe the complexities of the sound pressure field.

The SAFE method converges towards the exact solution of the governing equation and so in principle the method is accurate in both the near and the far field. This can be observed in Figs. 2 and 3, where the sound pressure field is continuous at $x = 0$, even at heights above the sound source. This is not the case for the PE method, as this method projects forward from the point source and even for extra wide angle predictions the method is not continuous over the line $x = 0$, and so the method is only an approximation in the near field. And of course, ray theory cannot be expected to capture the sound pressure field close to the point source. Thus, the SAFE method provides a benchmark solution for both the near and the far acoustic fields.

In practical sound propagation problems, it is common to want to know the sound pressure field at a single point and over a range of frequencies. Accordingly, in Fig. 4 an example TL calculation is presented for 1/3 octave bands over a frequency range from 10 Hz to 1 kHz, for the temperature inversion shown in Fig. 1.

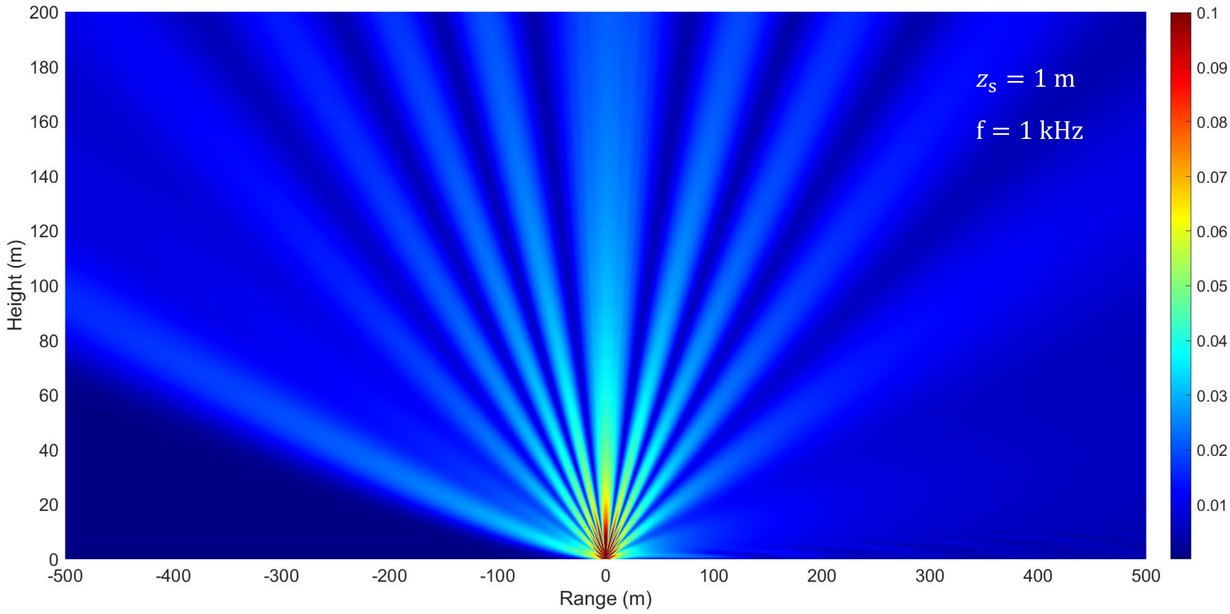

Figure 3: SAFE predictions of normalised sound pressure field at 1 kHz.

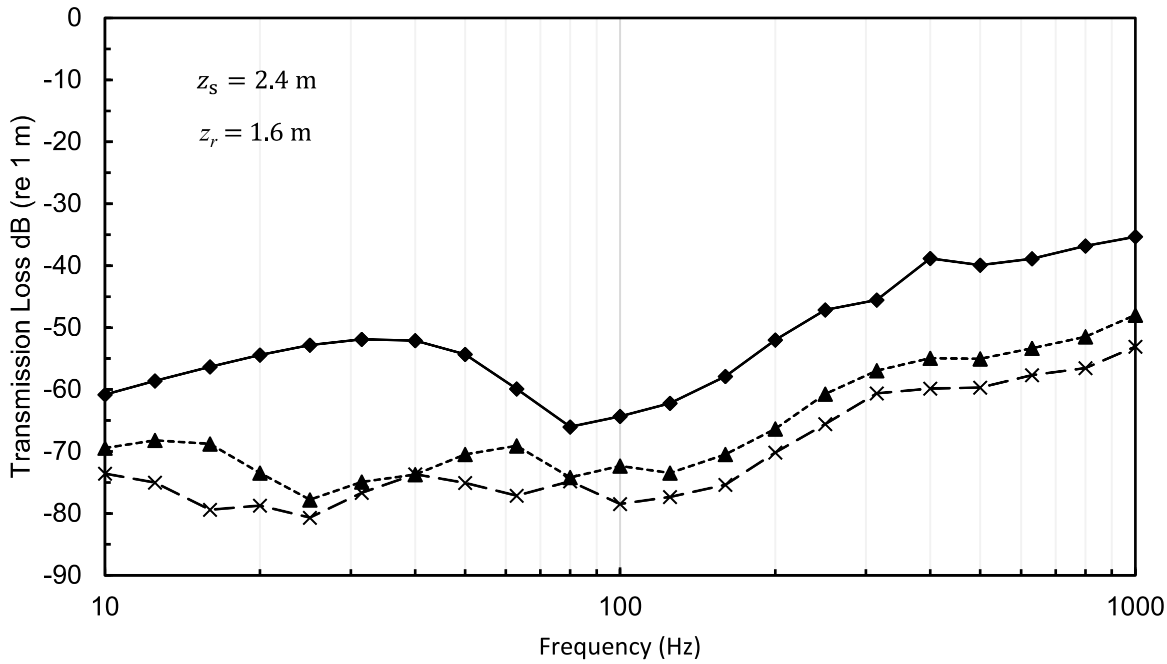

Figure 4: SAFE predictions of TL for a temperature inversion.
, $x_r = 500$ m; , $x_r = 2$ km; , $x_r = 3$ km.

Figure 4 illustrates that the SAFE method is capable of covering a relatively wide frequency range for what is a large computational problem. However, the method does of course require more elements once the characteristic wavelength becomes shorter, and this means that when the frequency is increased the solution time also increases. This is the trade-off for obtaining highly accurate predictions, and for Fig. 4 the solution time is greater than 24 hours. Clearly, this is not fast enough for use in an iterative design environment, however it is important to remember that this is a very complex problem and a height of at least 300 m is studied in this particular example. If the atmospheric conditions were simplified, and/or at higher frequencies it was acceptable to limit the predictions to lower heights, then it is possible to significantly reduce solution times, as well as study higher frequencies.

The development of a model that accommodates complex atmospheric conditions is designed to enable the analysis of sound propagation in Australia. This includes the analysis of noise from mines, especially at night time where other outdoor sound propagation models have been shown to provide inconsistent solutions for Australian conditions (Bullen, 2012). Other important areas include noise from wind turbines, where the SAFE model would enable sensitivity to atmospheric conditions to be studied. For example, Hansen et al. (2019) examined noise from wind turbines in South Australia using a ray based model to estimate the difference between sound pressure levels measured at 1.5m and at the ground surface. This was designed to compute a correction factor to enable measurements to be taken on the ground rather than in windy environments. However, this relies on a ray based model which contains a number of approximations. The advantage of the current approach is that all of these approximations are removed and predictions can be compared with measurements in the knowledge that any discrepancies are caused by the lack of information regarding the physical properties of the problem, rather than the model itself. To illustrate this, in Figs. 5 and 6, SAFE predictions are compared against the ray based predictions of Hansen et al. (2019), as well as the experimental measurements they report for the noise emitted by wind turbines. In these figures, $\Delta L_p = 20\log_{10}|p(x_r, 1.5)/p(x_r, 0)|$, where x_r is the range of the receiver.

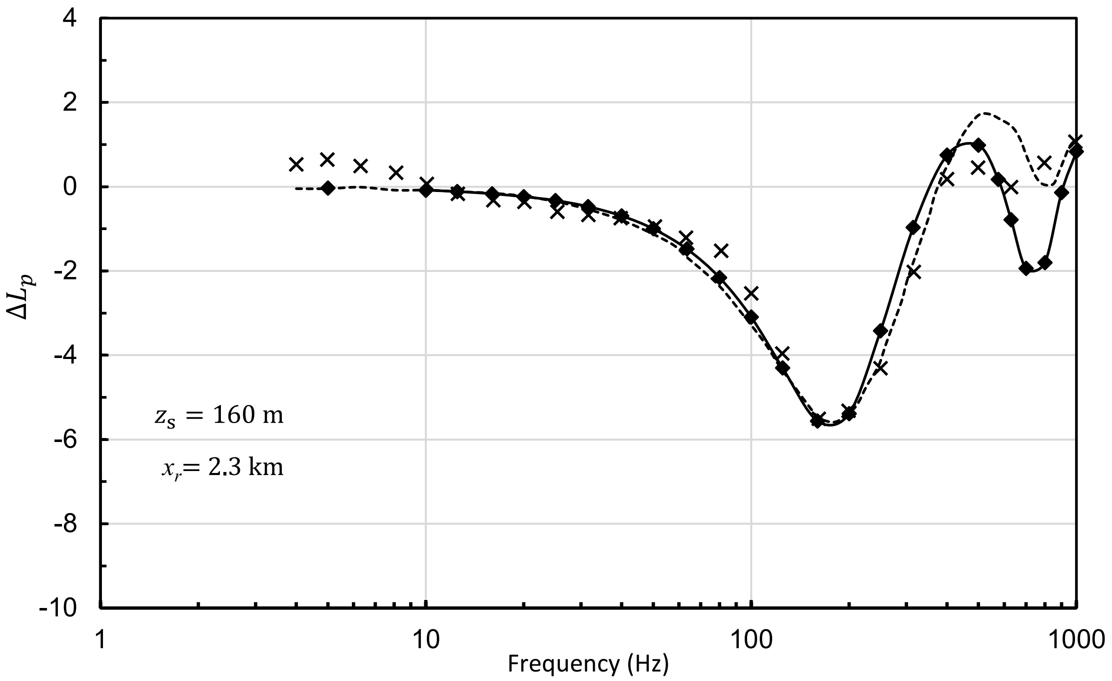

Figure 5: Predictions of ΔL_p for noise from a wind turbine, see Hansen et al. (2019).
, X , experiment; --------- , ray tracing model; —◆— , SAFE Model.

Figure 5 generally demonstrates good agreement between the ray and SAFE models, although some discrepancies begin to appear as the frequency is increased. In Fig. 6 these differences become more significant across the frequency range. Hansen et al. (2019) do not provide any information of the temperature profile for these measurements and so a simple logarithmic profile is chosen here, similar to the one seen in Fig. 1. However, it is expected that the wind effects will dominate and so the effective wind speed used by Hansen et al. (2019) is chosen to be similar to the one used in this study. Of course, some differences in the fluid properties will remain, and this may explain some of the differences observed between the two predictions for Fig. 6. In addition, it is possible that some of the approximations used by Hansen et al. are less successful for the geometry in Fig. 6

when compared to Fig. 5. Nevertheless, the SAFE model is seen to be closer to the experimental measurements at lower frequencies in Fig. 6, although some discrepancy is still evident. However, the advantage of an exact solution is that one can now conclude that this discrepancy is down to a lack of information regarding the atmospheric conditions and/or the ground impedance. Of course, it is also possible that range dependent effects may cause some of these discrepancies at higher frequencies, although given that these figures report a comparison between two predictions/measurements 1.5 m apart, this is not considered to be a significant source of discrepancy.

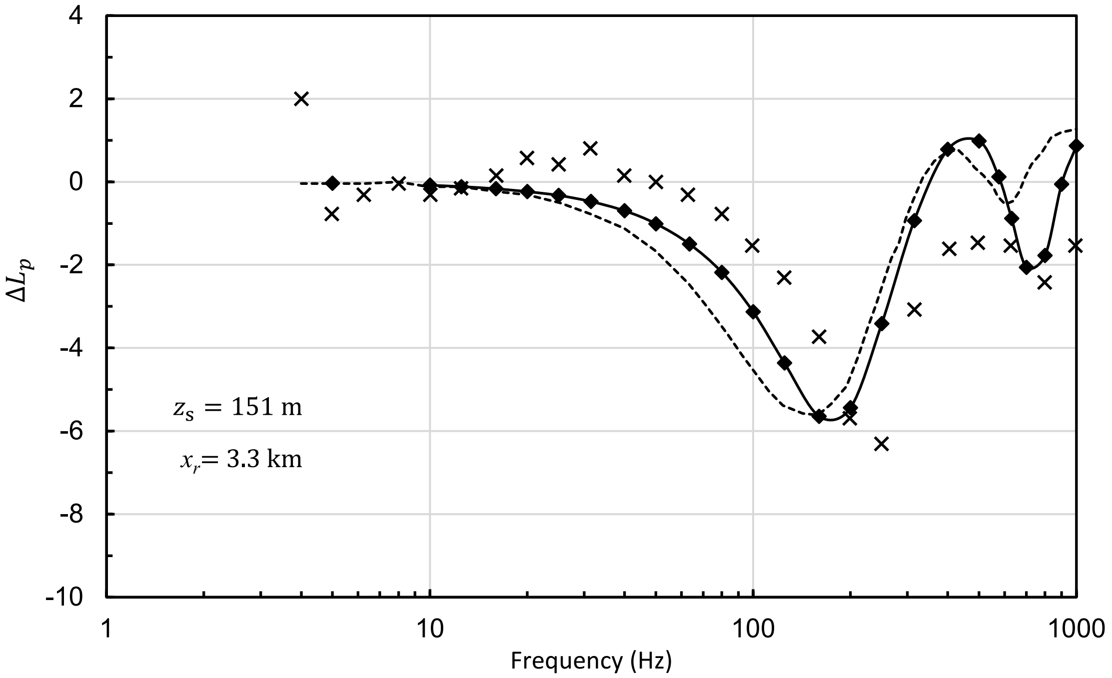

Figure 6: Predictions of ΔL_p for noise from a wind turbine, see Hansen et al. (2019).
, X , experiment; --------- , ray tracing model; —◆— , SAFE Model.

4 CONCLUSIONS

The use of a finite element based approach to compute outdoor sound propagation was investigated in this article. It is shown that by adopting a two dimensional approach in which the atmospheric conditions are assumed to be stratified in the vertical direction, a SAFE method can be applied that accommodates all of the physics of the problem. This enables the development of a method that converges towards the exact solution for complex atmospheric conditions, provided the problem remains range independent. Predictions are presented for a logarithmic wind velocity profile, as well as a temperature inversion with a logarithmic profile close to the ground. Predictions of complex sound pressure fields are generated over large distances and it is shown that the method can provide an insight into the sound pressure patterns at different frequencies. Furthermore, the method is shown to be able to accommodate complex atmospheric conditions often found in Australia.

The SAFE method is capable of providing accurate benchmark predictions for range independent problems. In principle, provided a sufficient number of finite elements and normal modes are included, the method will converge towards the exact solution, even at higher frequencies. However, as the size and upper frequency of the problem increases, the computational demands of the method will increase significantly so that the method will begin to slow down, especially above 1 kHz. The speed of solution is largely determined by the height of the problem to be analysed, and in this article the method was examined using a temperature inversion up to 300 m in height. For climatic conditions that do not require analysis up to such heights, it is possible to speed up the method significantly and to obtain solutions up to higher frequencies. Of course, it is also possible to speed up solution time by working with bigger computing power.

The SAFE method is currently limited to range independent problems. However, it is possible to adapt the model to study range dependent problems, such as the scattering from hills and sound barriers. This can be achieved by mapping the normal modes onto a full (two dimensional) finite element based solution of the region surrounding a range dependent feature, such as a hill or barrier. If the range dependent feature is relatively short in length when compared to the overall size of the problem, this should not significantly extend the solution time. This is because solution time is largely dominated by the solution of the eigenproblem to find the normal modes. This is especially true for items such as noise barriers, where mapping normal modes onto a small finite element discretisation surrounding the barrier will incur minimal additional computational expenditure. Similar observations also apply to wind turbines, where one can develop a sophisticated computational model for the mechanisms of noise generation close to the wind turbine, and then map this on to the SAFE method in order to project solutions into the acoustic far field. Thus, the SAFE method presented here provides a route to the development of accurate predictions for complex noise propagation problems, where it is important to include all of the relevant atmospheric conditions.

REFERENCES

Attenborough, K., Taherzadeh, S., Bass, H.E., Di, X., Raspet, R., Becker, G.R., Güdesen, A., Chrestman, A., Daigle, G.A., L'Espérance, A., Gabillet, Y., Gilbert, K.E., Li, Y.L., White, M.J., Naz. P., Noble, J.M. and van Hoof, H.A.J.M. (1995). "Benchmark cases for outdoor sound propagation models," *Journal of the Acoustical Society of America* 97, 173-191.

Bullen, R. (2012). "The Harmonoise noise prediction algorithm: Validation and use under Australian conditions", *Proceedings on Meetings of Acoustics 2012*, Freemantle, Australia.

Duan, W. and Kirby, R. (2019). "Guided wave propagation in buried and immersed fluid-filled pipes: Application of the semi analytic finite element method", *Computers and Structures*, 212, 236-247.

Duan, W., Kirby, R., Mudge, P. and Gan, T.-H. (2016). "A one dimensional numerical approach for computing the eigenmodes of elastic waves in buried pipelines", *Journal of Sound and Vibration*, 384, 177-193.

Gilbert, K.E. and White, J.K. (1989). "Application of the parabolic equation to sound propagation in a refracting atmosphere", *Journal of the Acoustical Society of America*, 85, 630-637.

Hansen, L.K., Zajamšek, B., Hansen, C.H. (2019) "Investigation of a microphone height correction for long-range wind farm noise measurements," *Applied Acoustics*, 155, 97-110.

Kirby, R. (2020) "Atmospheric sound propagation in a stratified moving media: Application of the semi analytic finite element method," *Journal of the Acoustical Society of America*, 148, 3737-3750.

Kirby, R. (2021) "Atmospheric sound propagation in a moving fluid above an impedance plane: Application of the semi analytic finite element method," *Journal of the Acoustical Society of America*, 149, 1285-1295.

Lihoreau, L., Gauvreau, B., Bérengier M., Blanc-Benon, P. and Calmet I. (2006). Outdoor sound propagation in realistic environments: Application of coupled parabolic and atmospheric models," *Journal of the Acoustical Society of America*, 120, 110-119.

Ostashev, V. E. and Wilson, D.K. (2016). *Acoustics in Moving Inhomogeneous Media*, 2nd Ed., Taylor Francis, New York

Ostashev, V. E., Wilson, D.K., and Muhlestein, M.B. (2020) "Wave and extra-wide-angle parabolic equations for sound propagation in a moving atmosphere," *Journal of the Acoustical Society of America,* 147, 3969-3984.

Taherzadeh, S., Li, K.M. and Attenborough, K. (1998) "Some practical considerations for predicting outdoor sound propagation in the presence of wind and temperature gradients," *Applied Acoustics*, 54, 27-44.

West, M., Sack, R.A. and Walkden, F. (1991) "The Fast Field Program (FFP). A second tutorial: Application to long range sound propagation in the atmosphere," *Applied Acoustics*, 33, 199-228.